LRP 393/90 January 1990

WAVE PROPAGATION AND ABSORPTION IN THE ELECTRON CYCLOTRON FREQUENCY RANGE FOR TCA AND TCV MACHINES

A. Cardinali

WAVE PROPAGATION AND ABSORPTION IN THE ELECTRON CYCLOTRON FREQUENCY RANGE FOR TCA AND TCV MACHINES

Alessandro Cardinali*

Centre de Recherches en Physique des Plasmas
Association Euratom - Confédération Suisse
Ecole Polytechnique Fédérale de Lausanne
21, Av. des Bains CH - 1007 Lausanne / Switzerland

Abstract

The main theoretical aspects of the propagation and absorption of electron cyclotron frequency waves are reviewed and applied to TCA and TCV tokamak plasmas. In particular the electromagnetic cold dispersion relation is solved analytically and numerically in order to recall the basic properties of mode propagation and to calculate the ray-trajectories by means of geometric optics. A numerical code which integrates the coupled first order differential ray-equations, has been developed and applied to the cases of interest.

* Permanent address: ENEA, Frascati

Introduction

Absorption of electron cyclotron frequency waves is a possible means of heating the TCV tokamak (under construction). They may also be used to assist the initial breakdown and to ramp the current [1]. A preliminary experiment to study the absorption of electron cyclotron waves for breakdown will be performed on TCA [1]. TCA is a small tokamak with central maximum magnetic field $B_0 = 1.5$ Tesla and inverse aspect ratio $\varepsilon \approx 0.3$.

Studies on sawtooth stabilization, breakdown, second and third harmonic heating can be performed by injecting radio-frequency waves, produced by a gyrotron operating at a frequency of 39 GHz and a power of 200 - 300 kW for 100 ms [2].

The main features of the propagation of radio frequency waves into the plasma can be deduced by the study of the dispersion relation and the solution of the ray-equations. Developed computer codes can be run with varied plasma and antenna parameters to yield useful information, which can subsequently be used to plan electron cyclotron experiments on TCA. Such information includes the choice of frequency, the mode polarization (O- or X-mode), the localisation of the harmonic and power deposition profile.

The plan of the paper is the following: in Section I we recall the main features of the electron cyclotron waves in plasmas by studying the cold electromagnetic dispersion relation in slab geometry. The best choice of frequency, polarization of the mode and angle of injection with the magnetic field is deduced for a target plasma (density, temperatures, magnetic field and so on) close to that of TCA.

In Section II the ray-tracing equations for E.C.W. are introduced and the effects of bidimensional geometry on the propagation are also shown. Absorption of the fundamental harmonic can be analysed by calculating the imaginary part of the dispersion relation for finite temperatures (finite Larmor radius expansion). Numerical applications to TCA plasmas are given. Finally, in the conclusions, possible extensions of this work are discussed.

I The Dispersion Relation for Electron Cyclotron Waves

Many of the features of E.C.W. propagation in tokamak plasmas can be deduced in a simple manner by studying the "dispersion relation" for electromagnetic waves at such frequencies (10 - 100 GHz) in cold stratified plasmas.

The derivation of the general "dispersion equation" has been reported in several text books [3, 4, 5] under the assumption that the plasma is uniform, stationary and unbounded. Under such an hypothesis the Maxwell-Vlasov system of equations can be Fourier analysed and the characteristics of the wave propagation can be deduced by studying the resulting dispersion equation, which links the wavevector $\mathbf{k}$ to the frequency ω. The dispersion relation for waves in the range of electron cyclotron frequencies reads [4]:

$$a n_\perp^4 + b n_\perp^2 + c = 0 \qquad (1)$$

where

$$\begin{aligned} a &= \varepsilon_{11} \\ b &= (n_\parallel^2 - \varepsilon_{11})(\varepsilon_{11} + \varepsilon_{33}) - \varepsilon_{12}^2 \\ c &= \varepsilon_{33}[(n_\parallel^2 - \varepsilon_{11})^2 + \varepsilon_{12}^2] \end{aligned} \qquad (2)$$

and

$$\varepsilon_{11} = 1 - x^2/(1-y^2)$$
$$\varepsilon_{12} = ix^2y/(1-y^2)$$
$$\varepsilon_{33} = 1-x^2 \qquad (3)$$
$$[x = \omega_{pe}/\omega,\ y = \Omega_{ce}/\omega] .$$

The ε_{ij} are elements of the dielectric tensor, while $n_\perp = k_\perp c/\omega$, $n_\parallel = k_\parallel c/\omega$ are respectively the refractive indeces perpendicular and parallel to the static magnetic field B_0 (note that the plasma is anisotropic owing to the presence of B_0), ω_{pe} and ω_{ce} are the electron plasma and electron cyclotron frequencies, which depend on the plasma density, n, and magnetic field, B_0, respectively. Assuming a stratified plasma and a non-uniform magnetic field, n and B_0 will be function of the x-coordinate (slab variable). In this case the solution of Eqn. (1) will relate the perpendicular wavenumber to the slab variable.

The coefficients in Eqns (2) of the dispersion relation do not depend on $n_\perp$ and hence the plasma is not spatially dispersive; Eqn (1) gives two independent solutions which correspond to two characteristic waves that can propagate in the medium. For spatially dispersive media there may be more than two solutions to Eqn (1).

The parallel wavenumber which appears in Eqn (2) is determined by the angle between the antenna and the direction of the magnetic field:

$$n_\parallel = \mathbf{n} \bullet \mathbf{B}/|\mathbf{B}| = |\mathbf{n}| \cos\varphi \qquad (4)$$

The damping of the propagating wave can be calculated everywhere in the plasma by considering the anti-hermitian part of the dielectric tensor. In the cold plasma case the anti-hermitian part of the dielectric

tensor is zero and the wave is not damped. Thermal corrections must be included to obtain the spatial damping rate, which reads [6, 7, 8]:

$$\gamma = \frac{\mathrm{Im}(D)}{|v_g|\left(\frac{\partial \mathrm{Re}(D)}{\partial \omega}\right)} \qquad (5)$$

where D (dispersion function) $\equiv D^{Real} + iD^{Imag.}$ and $|\mathbf{v}_g|$ is the group velocity along the x-direction. The rate of the power lost by the wave is

$$P_L(x) = \exp\left(-2\int_0^x \gamma dx\right) \qquad (6)$$

(In Eqn (5) D^{real} is given by L.H.S. of Eqn. (1) while in the integral of Eqn. (6) x = 0 and x = 1 represent the plasma centre and periphery respectively).

We deduce some of the main characteristics of electron cyclotron wave propagation in cold plamas by solving the dispersion equation (Eqn (1)) in the case of totally perpendicular injection ($k_{||} = 0$). As mentioned before Eqn. (1) has two solutions which correspond to two independent waves; they can be expressed in a very simple form:

$$n_\perp{}^2{}_x = (\varepsilon_{11}{}^2 - |\varepsilon_{12}{}^2|) / \varepsilon_{11} = [(1 - x^2)^2 - y^2] / (1 - y^2 - x^2)$$
$$n_\perp{}^2{}_o = \varepsilon_{33} = 1 - x^2 \qquad (7)$$

where the suffixes x and o mean extraordinary and ordinary mode respectively. The O-mode is also called "slow wave" and the X-mode "fast wave" referring to the phase velocity [Stix, 1962].

The "cut-off" of the O-mode ($n_\perp \rightarrow 0$) is at the point where:

$$\varepsilon_{33} = 1 - x^2 = 1 - \omega^2_{pe} / \omega^2 = 0 \qquad (8)$$

while that of the X-mode is defined by

$$\varepsilon_{11}{}^2 = |\varepsilon_{12}{}^2| \equiv (1 - x^2)^2 = y^2 \qquad (9)$$

The O-mode has no resonance while the X-mode has the upper-hybrid resonance ($n_\perp \rightarrow \infty$) located at the point where:

$$\varepsilon_{11} = 0 \rightarrow \omega^2 = \omega^2_{pe} + \Omega^2_{ce} \qquad (10)$$

This behaviour is shown in Figs 1a), b), c) where $n^2_\perp$ is plotted as function of x (slab coordinate) for the two modes using TCA plasma parameters, for three different injection angles ($n_\parallel$ = 0; .5; 1). The frequency chosen is 39 GHz which corresponds to the case where the first electron cyclotron harmonic is located at x = .385 ($\omega = \Omega_{ce}$), with a central magnetic field B_0 = 1.55 Tesla.

In the case of perpendicular propagation, the electron cyclotron harmonic $\omega = \Omega_{ce}$ is a regular point for the ordinary and extraordinary wave, and no absorption is present. In the case of the ordinary wave this is due to the fact that the electric field is linearly polarized in the direction of the magnetic field (**E** // **B**) and the absorption can occur only when thermal effects are included. In the case of the extraordinary wave the electric field is circularly polarized perpendicular to the magnetic field, in the ion rotation direction, and no electron heating is produced as long as $n_\parallel$ remains equal to zero.

This absence of absorption can be better understood when we calculate explicitly the imaginary part of $n_\perp$ (which gives the rate of absorption) for temperature and parallel wavenumber different from zero.

The damping rate for the ordinary mode is:

$$\gamma_O \approx \frac{1}{2}\frac{\omega_{pe}^2}{\Omega_{ce}^2}\frac{(1-\omega_{pe}^2/\omega^2)^{1/2}}{n_{||}^3}\frac{(1-\Omega_{ce}^2/\omega^2)^2}{\bar{v}_{the}}\sqrt{\pi}\bullet\exp\left[-\left(\frac{1-\Omega_{ce}/\omega}{n_{||}\bar{v}_{the}}\right)^2\right] \qquad (11)$$

and for the extraordinary mode:

$$\gamma_X \approx \sqrt{\pi}\frac{\omega_{pe}^2}{\omega^2}\frac{1}{n_{||}\bar{v}_{the}}\left(2-\frac{\omega_{pe}^2}{\omega^2}\right)^{-1/2}\exp\left[-\left(\frac{1-\Omega_{ce}/\omega}{n_{||}\bar{v}_{the}}\right)^2\right] \qquad (12)$$

where $\bar{v}_{the} = v_{the}/c$.

It is easy to see that for $n_{||} = 0$ or $v_{the} = 0$ both γ_o and γ_x are zero and no absorption is present. The maximum absorption for the X-mode is given at the point where $\omega = \Omega_{ce}$. The absorption of the ordinary wave is localized somewhat out of resonance. It is to be noted that the relativistic Doppler effect, which is not included in the dielectric tensor that we have used for our investigation, allows a small but non zero absorption even at $k_{||}=0$ and the Eqns (11) and (12) must be adjusted for $n_{||}<v_{the}/c$ [9,10,11,12].

To illustrate the propagation of the ordinary and extraordinary mode in slab geometry we have run our code for plasma parameters typical of TCA tokamak. The main characteristics of perpendicular propagation are recovered and the role of the cut-offs, resonances and cyclotron harmonics is pointed out.

Coming back to Figs 1a), b), c) where we have shown the dispersion curves for the O and X-modes for different $n_{||}$ values at the antenna, we can see that the plasma density has been chosen such that the cut-off of the O-mode is at the centre; in this case the O-mode propagates to the centre. For the X-mode, the dispersion curve shows the cut-off placed in the very edge of the plasma and somewhat more inside the upper hybrid resonance occurs. It is obvious that if one wants to excite the X-mode, the only possibility for reaching the E.C. resonance is to launch the waves from the high field side of the tokamak. Note that, in the examples of Fig. 1, the E.C. resonance, where the maximum absorption is located, has been placed at x = 0.385.

II Ray Tracing for E.C. Waves

The ray-tracing technique for studying the propagation and absorption of electromagnetic waves in the range of the electron cyclotron frequency relies on the WKBJ approximation of Maxwell's equations. This mathematical tool has been used extensively to study wave propagation in plasmas, and a large bibliography is available [13 - 22]. Here we present the ray-tracing equations for the position, wave number and amplitude of the wave and give numerical solutions of both the X and O-modes. This would provide some general indications of the wave propagation and absorption features in three-dimensional geometry.

The ray equations read:

$$\frac{d\mathbf{r}}{d\tau} = \frac{\partial D}{\partial \mathbf{k}}, \qquad \frac{d\mathbf{k}}{d\tau} = -\frac{\partial D}{\partial \mathbf{r}}, \qquad \frac{dt}{d\tau} = -\frac{\partial D}{\partial \omega}, \tag{13}$$

which are in the form of the Hamilton equations in classical dynamics. D is the hamiltonian of the system and in our case is the dispersion relation function for E.C. waves in plasmas (Eqn. (1)).

We now introduce a toroidal geometry (r, θ, φ) where r, θ, φ are the radius and the poloidal and toroidal angles respectively, and (k_r, m_θ/r, n_φ/R_0h_s) are the canonically associated wavenumbers (R_0 is the major radius and $h_s = (1 + r/R_0 \cos\theta)$). The ray-equations (13) can then be written in the following manner:

$$\frac{d\hat{r}}{d\tau} = \frac{\partial D}{\partial n_r}, \quad \frac{d\theta}{d\tau} = \frac{\partial D}{\partial m_\theta}, \quad \frac{d\varphi}{d\tau} = \frac{\partial D}{\partial n_\varphi}, \tag{14}$$

$$\frac{dn_r}{d\tau} = -\frac{\partial D}{\partial \hat{r}}, \quad \frac{dm_\theta}{d\tau} = -\frac{\partial D}{\partial \theta}, \quad \frac{dn_\varphi}{d\tau} = -\frac{\partial D}{\partial \varphi} = 0 \tag{15}$$

where $\hat{r} = r\,\omega/c$.

These equations must be integrated numerically after specifying the derivatives in the right hand side of the system (14) - (15), by using the hamiltonian given by Eqn. (1). The perpendicular and parallel wavenumbers in Eqn. (1) are related to k_r, m_θ/r, n_φ/R by the following equations:

$$n_{\|} = \mathbf{n} \bullet \frac{\mathbf{B}}{B} = \frac{m_\theta}{\hat{r}}\frac{B_\theta}{B} + \frac{n_\varphi}{\hat{R}}\frac{B_\varphi}{B}, \tag{16}$$

$$n_\perp^2 = n^2 - n_{\|}^2 = n_r^2 + n_x^2, \tag{17}$$

$$n_\chi = \frac{m_\theta}{\hat{r}}\frac{B_\varphi}{B} - \frac{n_\varphi}{\hat{R}}\frac{B_\theta}{B}. \tag{18}$$

The poloidal and toroidal magnetic field are related via the safety factor:

$$q(r) = \frac{r}{R_0}\frac{B_\varphi(r)}{B_0(r)} \tag{19}$$

A numerical ray-tracing code has been developed which integrates Eqns. (14) - (15). For the numerical integration, initial conditions must be given on the initial surface r = a. The two branches of the dispersion relation (mode O or X) can be followed and the pattern of wave propagation obtained in toroidal geometry showing the effect of density and magnetic field variation.

In Figs 2 and 3 we show ray-trajectories for the X-mode (top launch injection) for the different angles of injection (Figs 2a), b) and c)) and different values of the central density (Figs 3a), b) and c)). Near the X-mode cut-off the ray suffers a radial reflection. The wave absorption is calculated along the ray trajectories in an approximate manner by using Eqn. (5) [22-23].

In this case it is necessary to include in the code an expression for the imaginary part of D in terms of the elements of the dielectric tensor. The group velocity defined as:

$$\mathbf{v}_g = \frac{d\mathbf{r}}{dt} = -\frac{\partial D/\partial \mathbf{k}}{\partial D/\partial \omega}, \tag{20}$$

can also be calculated in the code. At the next order in the WKB approximation it is possible to find an equation for the amplitude of the electric field or, equivalently, the Poynting vector [15]:

$$\nabla \bullet \mathbf{S}_{k,\omega} = -2\gamma_{k,\omega} |\mathbf{E}_{k,\omega}|^2 \qquad (21)$$

where:

$$S_{k,\omega} = \frac{c}{8\pi} \mathrm{Re}\,(\mathbf{E}^*_{k,\omega} \times \mathbf{B}_{k,\omega}) - \frac{\omega}{8\pi} \mathbf{E}^*_{k,\omega} \bullet \frac{\partial \varepsilon^H}{\partial k} \bullet \mathbf{E}_{k,\omega}$$

$$\gamma_{k,\omega} = \frac{\omega}{16\pi} \mathbf{e}^*_{k,\omega} \bullet \varepsilon^A \bullet \mathbf{e}^*_{k,\omega} \qquad (22)$$

The solution of this equation enables us to compute the power deposition profile inside the plasma.

In Fig 4 we have plotted the values of γ in function of the radius for the cases of Figs 2a), b) and c). In the vicinity of the E.C. resonance (x=0.385) the ray is strongly absorbed.

Conclusions

An analysis of electron cyclotron wave propagation in slab and toroidal geometry) has been performed. The main characteristics of the propagation and absorption have been calculated for the case of TCA tokamak by using a ray-tracing code for a maxwellian plasma of circular cross-section. An extension to non-circular and D-shaped equilibria could also be possible by connecting our code to an equilibrium code. Using the ray tracing code it would then be possible to plan heating on a tokamak experiment and to predict some features of the absorption.

Acknowledgement:

The author would like to acknowledge here the fruitful and stimulating collaboration within the CRPP in particular Prof. F. Troyon and Dr. A. Pochelon for their valuable discussions and encouragement and Mr. Ph. Marmillod for the computer assistance.

This work was partly supported by the Fonds National Suisse de la Recherche Scientifique.

References

[1] A. Pochelon, private communication, Lausanne June 1988

[2] A. Pochelon, Comptes rendus of the scientific meeting, Lausanne, August 1988,

[3] T.H. Stix, The Theory of Plasma Waves, M. Graw-Hill, N.York, 1962

[4] D.C. Montgomery, D.A. Tidman, Plasma kinetic Theory, Mc Graw - Hill, N.Y, 1964

[5] Ginzburg V.L., Propagation of e.m. waves in plamas, Pergamon, Oxford, 1964

[6] Bornatici M., Cano R., De Barbieri O., Engelmann F., Nuclear Fusion 23, 1153, (1983).

[7] Litvak A.G., Permitin G.V., Suvorov E.V., Flajman A.A., Nucl. Fusion 17, 659, (1977).

[8] Alikaev V.V., Dnestrovskii Yu.N., Parail V.V., Pereverzec G.V., Sov. J. Plasma Phys. 3, 127, (1977).

[9] Bornatici M., Plasma Phys. 24, 629 (1982).

[10] Bornatici M., Ruffina U., Plasma Phys. 28, 1589 (1986).

[11] Bornatici M., Engelmann F., Lister G.G., Phys. Fluids, 22, 1664 (1979).

[12] Fidone I., Granata G., Meyer R.L., Ramponi G., Plasma Phys. 22, 203 (1980).

[13] Bernstein I.B., Physics of Fluids, 18, 320 (1975).

[14] Rukhadze A.A., Silin V.P., Soviet Phys. Uspelkhi, 7, 259 (1964).

[15] Brambilla M., Cardinali A., Plasma Physics 24, 1187, (1982).

[16] Bernstein I.B., Baldwin D.E., Phys. Fluids 20, 116, (1977).

[17] Tanaka S., Maekawa T., Terumichi Y., Hamada Y., IEE Transactions on Plasma Science Vol. PS-8 2 68 (1980).

[18] Batchelor D.B., Goldfinger R.C., Weitzner A., IEE Transactions in Plasma Science Vol. PS-8 2 78 (1980)

[19] D'Haeseleer W.D., Shohet J.L., Audenaerde V.R., IEE Transactions in Plasma Science Vol PS-8 15, 1 28, (1987).

[20] Bornatici M., Engelmann F., Comments Plasma Phys. Controlled Fusion 8, 57 (1983).

[21] De Luca F., Maroli C., Journal Plasma Phys. 90, 299 (1978).

[22] Airoldi A., Orefice A., Ramponi G., Il Nuovo Cimento, 6D, 527, (1985).

[23] Fidone I., Fichet M., Granata G., Meyer R.L., F.A.R. Internal Report EUR-CEA-FC-1124 (1981)

Figure captions

Fig. 1 : Dispersion relation : perpendicular refractiv index square $n_\perp^2$ for different injection angles a) $n_{||}=0$, $\varphi=90°$; b) $n_{||}=0.5$, $\varphi=60°$; c) $n_{||}=0.866$, $\varphi=30°$; d) $n_{||}=1$, $\varphi=0°$. The calculation is made for $x_{res}=0.385$ (f=39GHz, B=1.55T) and a density

$n_e(0)=1.886\cdot10^{19}m^{-3}$, corresponding to the 0-mode cut-off on axis.

Fig. 2 : X-mode top launch : $n_{||}$-scan : $n_{||}=0, \pm 0.5; \pm 0.866$ corresponding to toroidal injection angles $\varphi = 90°, \pm 60°, \pm 30°$ (39GHz, $x_{res}=0.385$) at $n_e(0)=2\cdot10^{19}m^{-3}$.

Fig. 3 : X-mode top lauch : density-scan : $n_e(0)=1,2,3,4,5\cdot10^{19}m^{-3}$, for $n_{||}=0$ and for $x_{res}=0.385$ (f=39GHz, B=1.55T).

Fig. 4 : Absorption coefficient $\gamma(m^{-1})$ for $\varphi=30°$ and 60° (cases of Fig. 2).

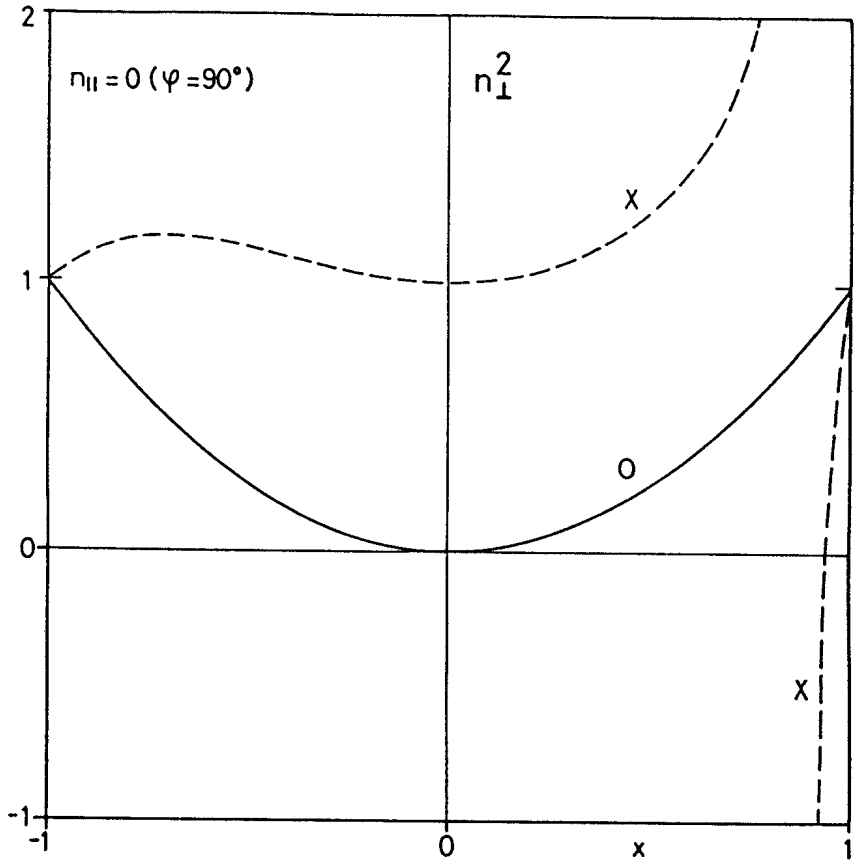
2
1
0
-1
-1
0
x
1
$n_{II} = 0\ (\varphi = 90°)$
$n_{\perp}^2$
X
O
X

Fig. 1a)

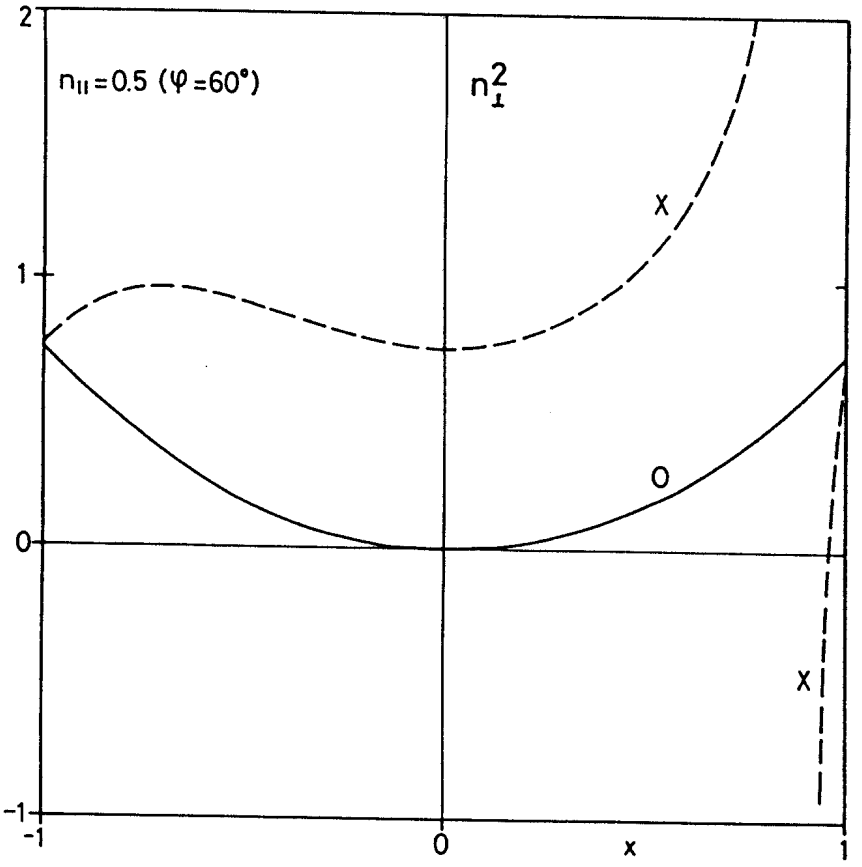
2
1
0
-1
-1
0
x
1
$n_{II} = 0.5\ (\varphi = 60°)$
$n_{\perp}^2$
X
O
X

Fig. 1b)

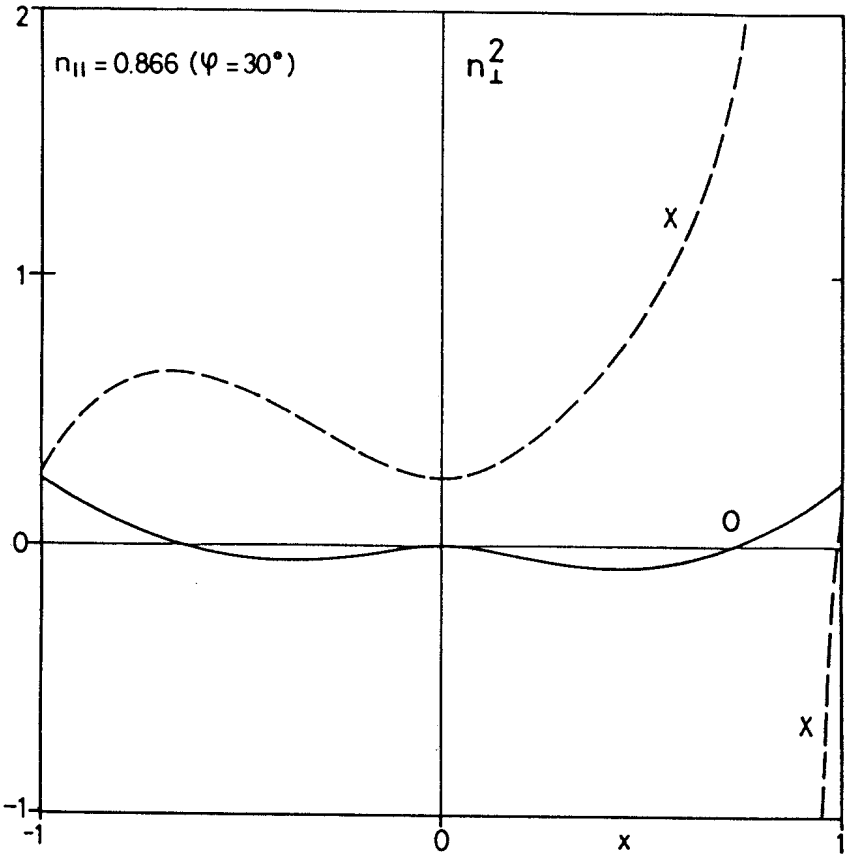
$n_{II} = 0.866$ ($\varphi = 30°$)
$n_\perp^2$
X
O
X
2
1
0
-1
-1
0
x
1

Fig. 1c)

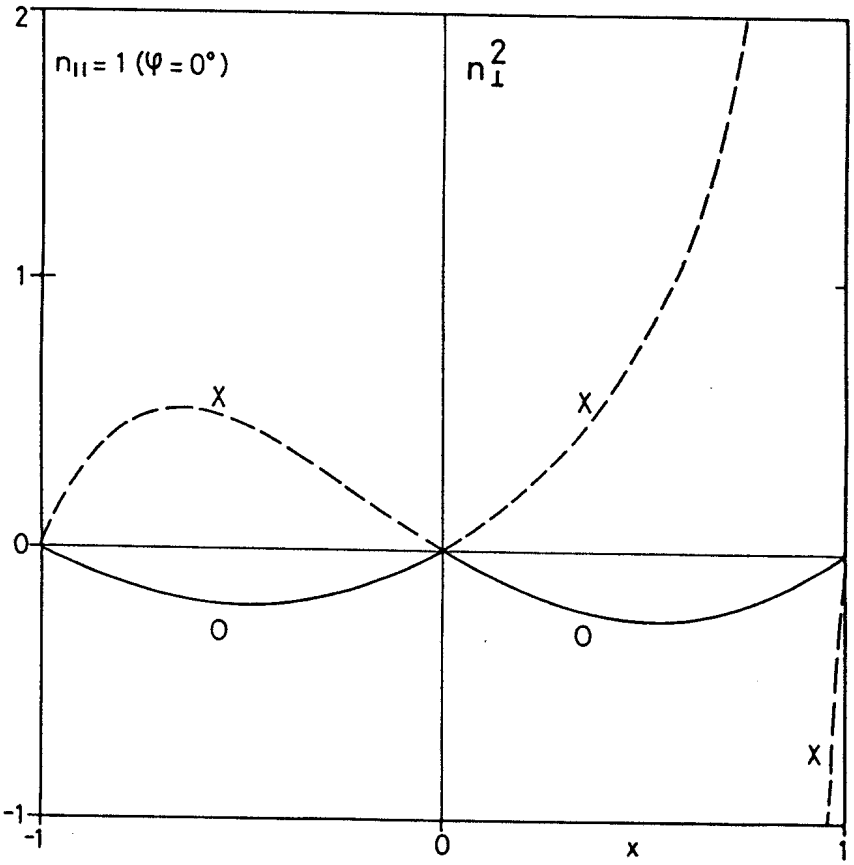
$n_{II} = 1$ ($\varphi = 0°$)
$n_\perp^2$
X
X
O
O
X
2
1
0
-1
-1
0
x
1

Fig. 1d)

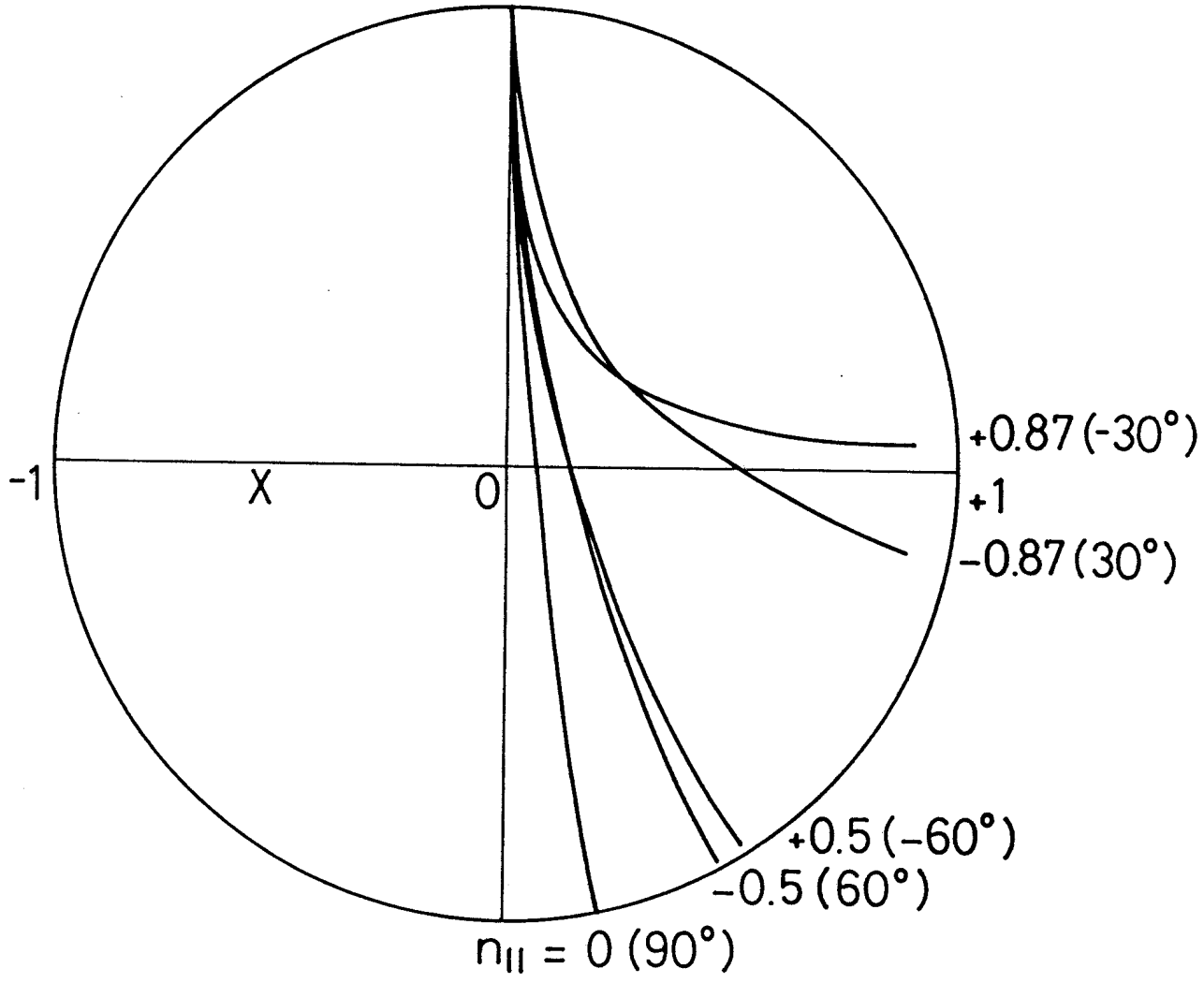

Fig. 2

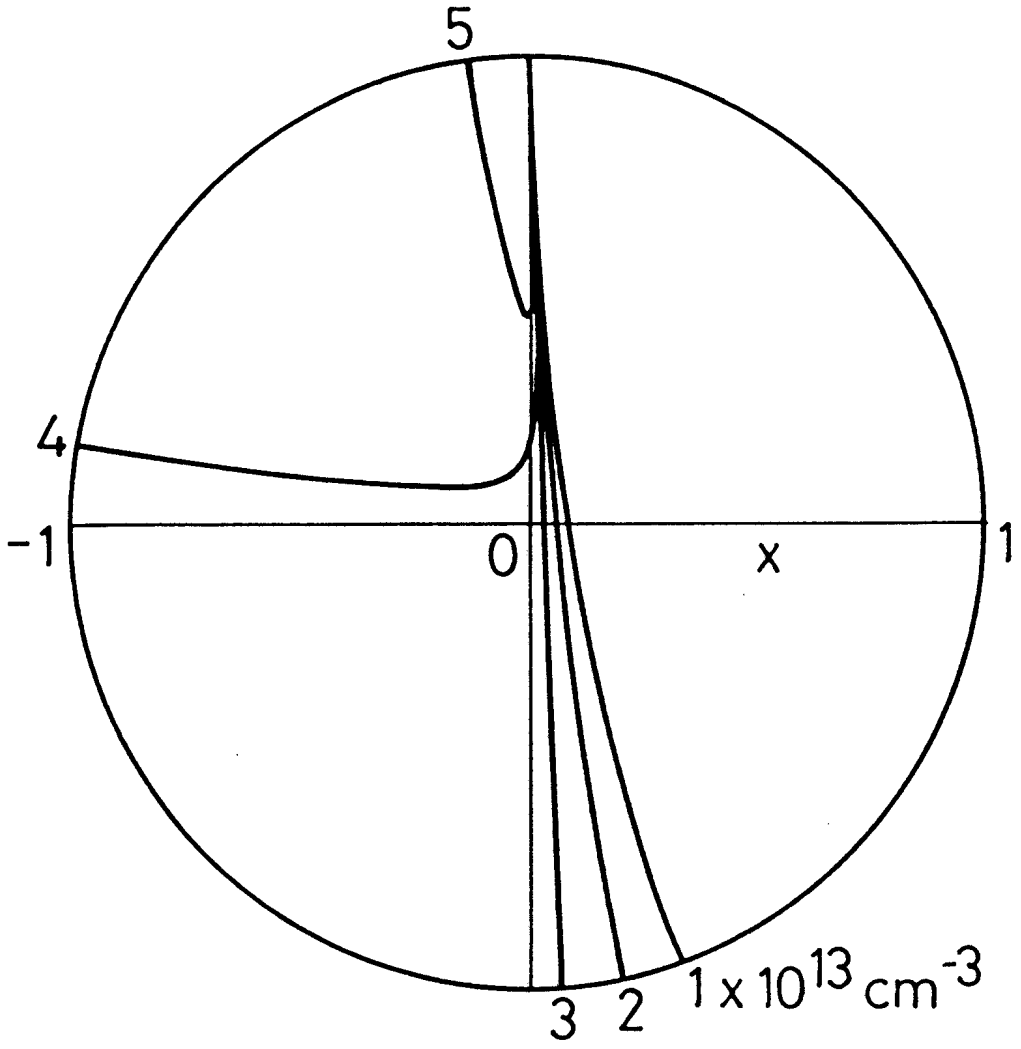

Fig. 3

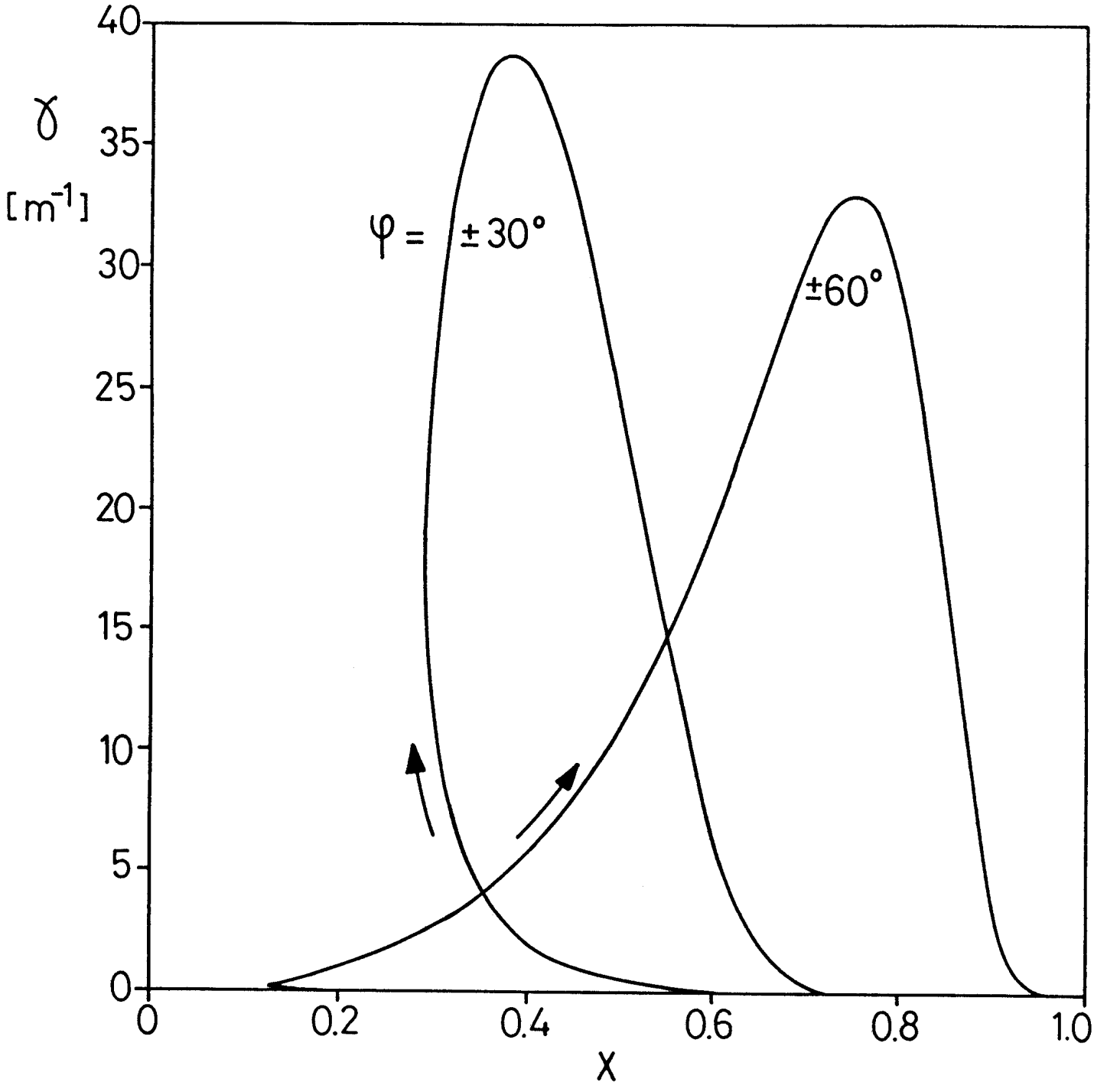

Fig. 4